6.5

IDEALIZED SIMULATIONS OF NOCTURNAL SEVERE WIND–PRODUCING CONVECTIVE SYSTEMS

Matthew D. Parker*
North Carolina State University, Raleigh, North Carolina

1. INTRODUCTION AND BACKGROUND

Organized convection has long been recognized to have a nocturnal maximum over the central United States. Many nighttime convective systems produce severe surface winds (Johns and Hirt, 1987), even though they often appear to be elevated above and decoupled from a stable nocturnal boundary layer. Recent work by Trier et al. (2006) has begun to address the mesoscale mechanisms that support long–lived elevated convective systems. However, the role of the stable boundary layer and its effects on the governing dynamics of convective systems' inflow and updraft trajectories still are largely unexplored. The present study uses idealized numerical simulations to investigate the mechanisms for the maintenance, propagation, and severe wind production of "elevated" convective systems.

A handful of mechanisms for the retriggering of elevated storms have been proffered, including gravity waves atop stable layers and larger–scale ascent associated with fronts or low–level jets. However, it is also possible that, despite the presence of a stable boundary layer, many nocturnal or cold–sector convective systems are not actually "elevated". In other words, they remain "surface–based" because they continue to ingest air with CAPE from the low–levels. A recent observational study of severe wind–producing convection by Kuchera and Parker (2006) suggested that, once a convective system has matured and produced a surface cold pool, it can continue lifting near–surface air despite its increased CIN (provided that the air still has CAPE). It is therefore possible that nocturnal convective systems may continue to be sustained by lifting at their outflow boundaries, and perhaps to produce severe winds through fairly well–known processes.

As a litmus test for the basic governing dynamics, the present numerical experiments use horizontally homogeneous initial conditions (i.e. they include neither fronts nor low-level jet streams). The ongoing simulations are meant to evaluate the preceding hypotheses and elucidate the key parcel trajectories and governing dynamics for "nocturnal–like" storms and their severe wind production.

**Corresponding author address:* Matthew D. Parker, Department of Marine, Earth, and Atmospheric Sciences, North Carolina State University, Campus Box 8208, Raleigh, NC 27695. E-mail: mdparker@ncsu.edu

2. METHOD

This work incorporates 2D and 3D simulations using version 1.10 of the nonhydrostatic cloud model described by Bryan and Fritsch (2002). In order to represent convective clouds, the simulations use ice microphysics and have horizontal grid spacings of 250 m, and a maximum vertical grid spacing of 250 m, which decreases progressively to 100 m below z=3500 m. The condensed grid in the lower troposphere improves the depiction of "nocturnal" stable layers in the model. The 2D simulations, reported here, use a grid that is 800 x 20 km; the 3D simulations (in progress and not reported here) use a grid that is 400 x 60 x 20 km. In both cases, the along–line dimension is periodic. In order to initiate convection the model includes an infinitely long, north–south linear warm bubble (+2K, with a relative humidity of 0.85); in the 3D case random temperature perturbations of up to 0.1K are added to ensure that 3D motions develop.

Although the full simulation matrix incorporates other soundings and wind profiles, the simulations described herein use the idealized Parker and Johnson (2004) midlatitude MCS sounding (PJ04), with linear u–wind shear below 3 km and constant wind thereabove. The control simulations have a shear vector magnitude of 18 m/s between the surface and 3 km.

Within some of the model runs, artificial cooling is added after 3 h of simulated time (around the time when the simulated squall line has reached maturity). The cooling is accomplished by defining a reference temperature,

$$T_{ref} = 301\,\mathrm{K} - (t - 3\mathrm{h}) \cdot 3\frac{\mathrm{K}}{\mathrm{h}}, \qquad (1)$$

and at each timestep setting the temperature at all points below 1 km AGL to be:

$$T = \min\left(T,\ T_{ref}\right). \qquad (2)$$

The net effect is the creation of an isothermal layer whose temperature decreases from the initial surface temperature (301 K) at a rate of 3 K/h; because T decreases with height in the initial condition, the stable layer is initially shallow, and grows slowly to its maximum depth of 1 km over the course of roughly 3 h. In various experiments the cooling is applied for between 3 and 9 hours in order to create stable layers of differing densities (Fig. 1). The approach mimics what occurs in the High Plains of the U.S. in that it enables the convection to mature in an afternoon–like sounding, and then to evolve as a nocturnal–like sounding develops.

3. RESULTS

To this point in time, the run–to–run sensitivities have been similar for the various soundings and wind profiles test; so, in the interest of brevity, only the constant shear PJ04 simulations are reported here. The PJ04 sounding is of interest because it is representative of the mean environment for MCSs in the central U.S., and because it has very little moisture above the mixed layer (not shown; interested readers should see Fig. 10 of Parker and Johnson, 2004). Because of this latter property, there is not an abundant source of moisture available for elevated storms: the most unstable parcels reside in the initial state's lowest levels. This provides perhaps the most stringent test of the requirements for nocturnal convection.

3.1 Control run

As summarized in Fig. 2, the control run produces a long–lived convective line with trailing stratiform (TS) precipitation. After briefly producing some line–leading precipitation, the system's surface outflow begins to intensify, its eastward motion commences, and its TS region develops. After roughly 2h, the surface outflow has a quasi–steady temperature deficit of 14-16 K, and continually produces peak surface winds between 25 and 40 m s^{-1}. The absolute magnitude of the wind gusts should not be used literally as it is partly a function of the idealized model configuration. However, for the sake of argument, within the model's dynamical world and the parameter space studied here, the control run constitutes a severe wind–producing squall line (gusts in excess of 50 kts, or roughly 23 m s^{-1}). This severe squall line is "surface–based". In other words, throughout its mature phase (i.e., after the first 2–3 hours) the updrafts comprise air from within the mixed layer in the lowest part of the troposphere. The convective line's signature is readily apparent from the high concentration of the passive 0-500 m tracer that is present at 3 km AGL (colored contours in Fig. 2).

3.2 Addition of cooling

When the 3 K h^{-1} cooling is applied after t=3h, the severe, surface–based squall line gradually evolves into a non–severe, elevated squall line. In the period from 3–6 hours, even though the lower levels are being stabilized, the simulated system continues to produce surface winds in excess of 30 m s^{-1} (Fig. 3). In addition, through t=6h the system in the stabilized environment continues to look like a healthy convective line with TS precipitation (top panel in Fig. 4). At this point, the cross-section of total hydrometeor content is almost identical to that for the control run (not shown). In short, the initial 9 K of surface cooling applied between 3 and 6 h does not appear to hinder the squall line much.

Thereafter, however, as the stability increases the surface winds begin to decrease, falling below "severe" levels after t=7h (Fig. 3). The decrease in surface wind speed is concurrent with the system's evolution away from being cold pool–driven. At t=6h there is still a large buoyancy gradient across the outflow's leading edge (Fig. 5), and the leading edge of the convection is intense and upright (Fig. 4). Low–level passive tracers launched below 1 km AGL (Fig. 6: red from 0-500 m and green from 500-1000 m) are all lifted abruptly at the outflow boundary. However, by t=7h, the surface outflow is not significantly colder than the cooled pre-line environment because T_{ref} has approached the outflow temperature (Fig. 3), and by t=8h, the characteristic density current shape of the outflow is no longer evident in the lowest 500 m AGL (Fig. 5).

This corresponds with the onset of "underflow" of the squall line: the passive tracer from below 500 m AGL (red in Fig. 6) is evident in much smaller concentrations in the system updrafts, and much of it begins to pass underneath the convective line without being lifted. Instead, during the window from t=8–10h, the convection is increasingly fed by air from farther aloft (green and blue in Fig. 6). The updrafts that correspond to significant condensate in the convective line are completely devoid of air from below 500 m after roughly t=9h (Figs. 3 and 6). In other words, the system has become truly elevated: it is cut off from the air in the lowest levels.

The fact that the convection survive for an additional 3+ hours in the simulation is a somewhat novel result. To the author's knowledge, elevated convection has never before been simulated in an idealized homogeneous model. In the present case, the mechanism for maintenance is a gravity wave atop the imposed stable layer. This gravity wave arises because the original cold pool head, which represents an upward bulge in the isentropes, extends above 1 km AGL and remains after the artificial cooling is imposed (Fig. 5). What was once a density current is converted into a gravity wave through erosion of its density anomaly over only part of its depth.

Interestingly, despite the removal of the outflow's density perturbation, the speed of the simulated convective system actually increases after t=9h (Fig. 3). The implication is that the transition from cold pool–driven system to gravity wave–driven system entails a change in propagation speed. Elsewhere in this volume, Billings and Parker (2006) consider an observed case that may exemplify this behavior. While the maintenance of the truly elevated system is interesting in its own right, the mechanisms for production and cessation of severe winds are also extremely important, and merit additional attention.

3.3 *Applying only limited cooling*

An important question is the degree to which the artificial cooling can be added without crossing the critical threshold at which severe winds cease. In the full cooling run (Fig. 3), the surface winds begin to diminish after T_{ref} has fallen by roughly 10K (around t=6h). If the cooling is halted once the surface has been cooled 10K, can the system continue producing severe winds, or has some irreversible downward trend already begun?

An additional experiment in which T_{ref} is only allowed to fall to 291 K reveals that the system is able to continue producing severe surface winds (Fig. 8). After applying the cooling, the degree of stabilization is considerable (Fig. 1; the green curve is a close approximation to the final state in the new "on/off" run). However, winds from 25–35 m s^{-1} persist. Several key differences between the "on/off" and "full" cooling cases bear emphasis.

First, the "on/off" system remains in the cold pool–driven mode, as opposed to the gravity wave–driven mode of the "full" system (cf. Figs. 3 and 8). This is manifest by the fact that T_{min} remains below T_{ref}, that the low level passive tracer continues to be ingested by the system updrafts, and that the forward speed of the system is constant throughout the simulation (Fig. 8). Perhaps as a consequence of its enduring cold pool forcing, the convection in the on/off simulation remains stronger and better organized than that in the full cooling simulation (not shown), which in turn appears to have consequences for the system's severe wind production.

In both the full and on/off cooling cases, the evolution is identical through 6h of simulated time. By t=4–6h, an intense rear inflow jet (RIJ) has developed beneath the TS precipitation region (Fig. 7). The severe surface winds are found in the zone where this rear inflow descends (i.e. warm colors at the surface in Fig. 7) as a consequence of hydrometeor loading and latent chilling just aft of the convective line. In the control and on/off simulations, the RIJ continues to develop westward through t=8h (middle panel of Fig. 7). In the on/off case, severe winds by t=8h are less widespread (a much smaller zone of descent to the surface in Fig. 7), but there are still places of locally intense evaporation and water loading that drive the high winds to the surface (the two small downdraft columns near x=450km in Fig. 7).

However, as the artificial cooling continues in the 'full" simulation, two differences appear. First, the RIJ becomes completely elevated by t=8h (bottom panel of Fig. 7); this is coincident with the onset of "underflow" by the near–surface air (Fig. 6). And second, the region of rear inflow becomes smaller and the rear–to–fore velocities become weaker (cf. middle and bottom panels in Fig. 7). In short, the on/off simulation illustrates that a modest increase in stability decreases the areal extent over which the RIJ descends. However, if the RIJ remains strong, it may still descend to the surface at isolated locations. As the the low–level stability is further increased, penetrative downdrafts become even less likely (i.e. air from above 500 m AGL is no longer present at the surface in the later stages of Fig. 6); and, as the system becomes disorganized, the RIJ also weakens so that any remaining penetrative downdrafts are less likely to be severe.

4. SYNTHESIS

The present simulations are part of an ongoing effort to understand nocturnal convective systems, which are common in the U.S. Some of the results are novel in that no larger scale front or low–level jet stream was required in order to sustain the simulated storms in an environment with a stable boundary layer. In the on/off cooling run, a reasonable amount of artificial low–level "nocturnal" cooling (10K, or 18°F) was applied and the convective system survived and produced uninterrupted severe surface winds. Analysis shows that this on/off system continued to be cold pool–driven and surface–based despite the increased low–level stability. With more extreme amounts of low–level cooling ($>$15K, or 27°F), the system became truly elevated, with underflow of low–level air. The elevated system was maintained by the lifting of mid–level air over a gravity wave atop the stable layer, and its motion and structure changed during the evolution from a cold pool–driven to a gravity wave–drive storm. In addition, as its rear inflow weakened and penetrative downdrafts were increasingly inhibited, the system ceased to produce severe winds.

The preceding results suggest that *many of the severe nocturnal convective systems that were previously thought to be "elevated" are actually "surface–based"*. Ongoing work, including 3D simulations and analysis of parcel trajectories, is aimed at a fuller dynamical understanding of these processes.

REFERENCES

Billings, J. M., and M. D. Parker, 2006: Evolution and maintenance of the 22-23 June 2003 nocturnal convection during BAMEX. Preprints, *23rd Conference on Severe Local Storms*, St. Louis, MO, Amer. Meteor. Soc., CD–ROM, P4.3.

Bryan, G. H., and M. J. Fritsch, 2002: A benchmark simulation for moist nonhydrostatic numerical models. *Mon. Wea. Rev.*, **130**, 2917–2928.

Johns, R. H., and W. D. Hirt, 1987: Derechos: Widespread convectively induced windstorms. *Wea. Forecasting*, **2**, 32–49.

Kuchera, E. L., and M. D. Parker, 2006: Severe convective wind environments. *Wea. Forecasting*, **21**, 595–612.

Parker, M. D., and R. H. Johnson, 2004: Structures and dynamics of quasi–2d mesoscale convective systems. *J. Atmos. Sci.*, **61**, 545–567.

Trier, S. B., C. A. Davis, D. A. Ahijevych, M. L. Weisman, and G. H. Bryan, 2006: Mechanisms supporting long-lived episodes of propagating nocturnal convection within a 7-day wrf model simulation. *J. Atmos. Sci.*, in press.

ACKNOWLEDGMENTS

The research reported here is supported by the National Science Foundation under Grant ATM–0349069 and ATM–0552154.

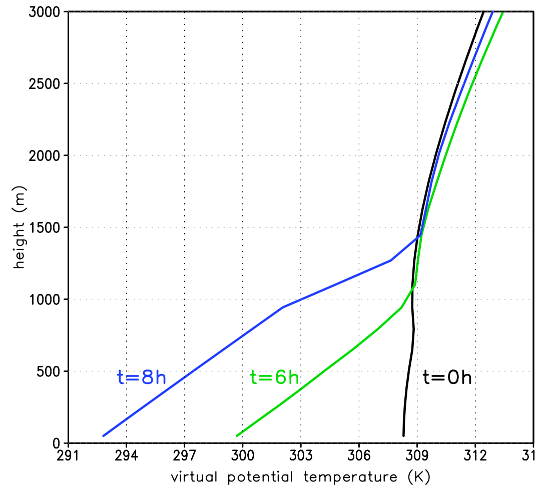

Figure 1: Profiles of virtual potential temperature for the pre–storm environment (i.e. on the eastern edge of the domain) for the base state (black), as well as for two times in the simulation with cooling (after 6 hours: green; after 8 hours: blue). Note that although the cooling was only applied below 1 km, θ_v also decreases slightly above 1 km by t=8h owing to vertical diffusion.

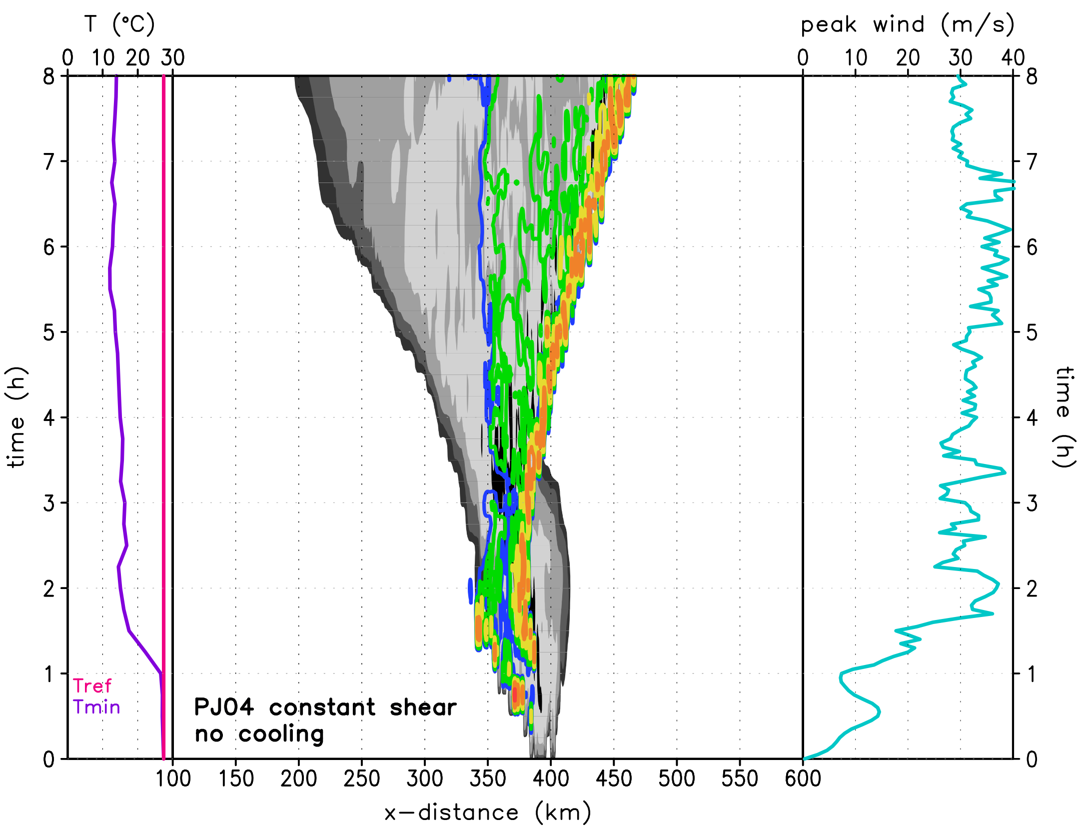

Figure 2: Behavior over time of the control simulation. The left panel depicts the change in time of T_{ref} (magenta; note that T_{ref} was constant in the control simulation) as well as the domain's minimal surface temperature (T_{min}, purple, a measure of the cold pool strength). The center panel is a Hovmoller diagram depicting the total hydrometeor mixing ratio at 6 km AGL (grayscale, shading at 0.005, 0.02, 0.08, 0.32, 1.28, and 5.12 g kg^{-1}) and the value of a passive low–level tracer (initial value=1 below 500 m AGL) at 3 km AGL (colored contours at 0.05, 0.1, 0.2, 0.4, and 0.8). The right panel depicts the change in time of the strongest surface wind perturbation in the model domain.

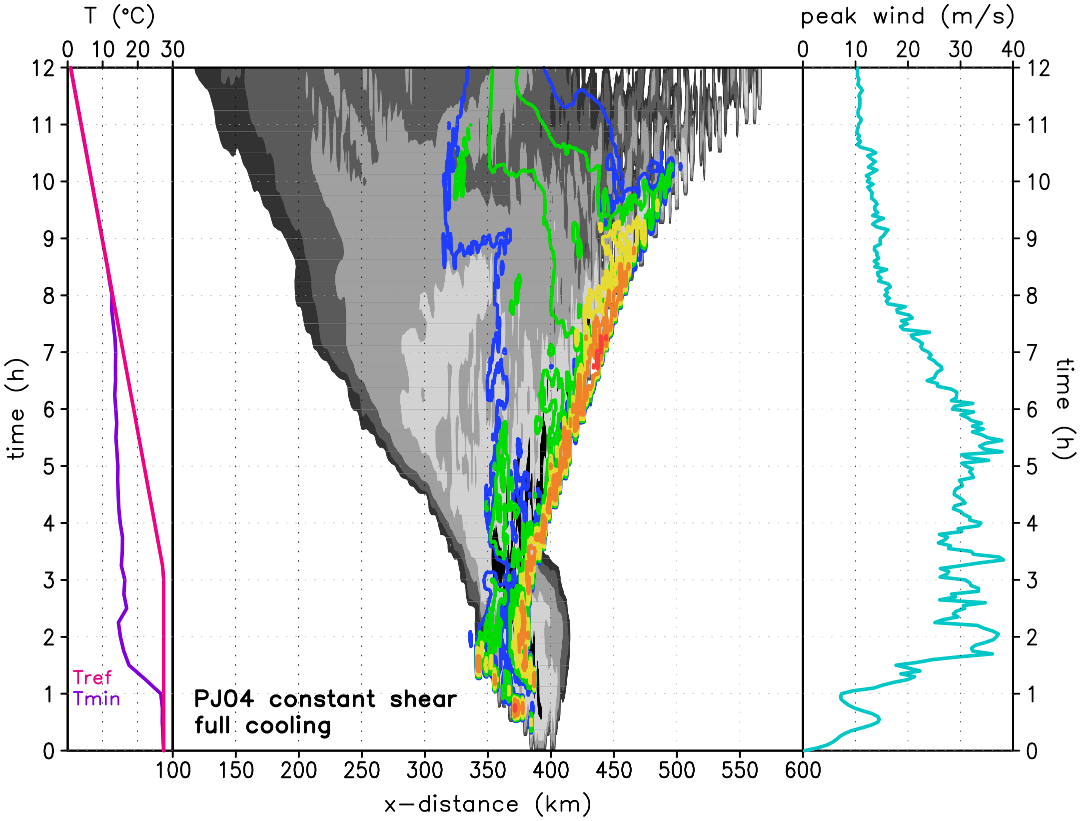

Figure 3: Same as Fig. 2 except for the run in which the 3 K h^{-1} cooling was applied after t=3h. Note that 12 hours are depicted (vs. 8h in Fig. 2).

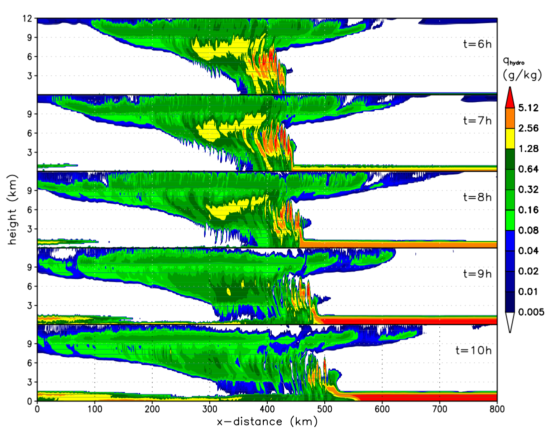

Figure 4: Cross-section of total hydrometeor mixing ratio, shaded as shown, at hourly intervals for the simulation with cooling applied (cf. Fig. 3). The elevated boundary layer values in advance of the squall line after t=7h represent a dense fog that develops in response to the artificial chilling.

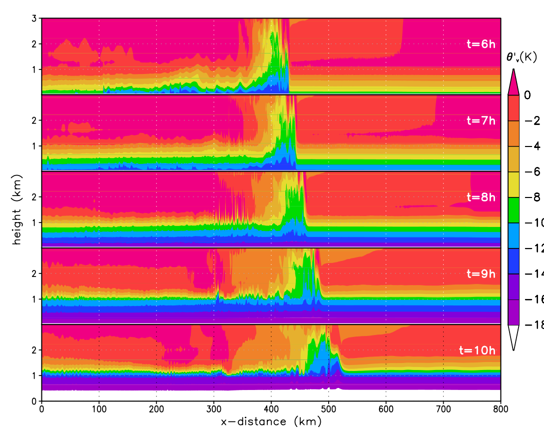

Figure 5: Same as Fig. 4 except for virtual potential temperature perturbation, shaded as shown.

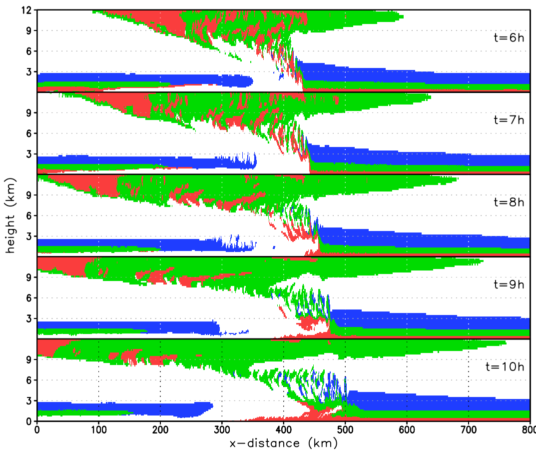

Figure 6: Same as Fig. 4 except for three passive tracers. Red: initially =1 below 500 m AGL. Green: initially =1 between 500 and 1000 m AGL. Blue: initially =1 between 1 km and 3 km AGL. If a grid box contains more sub–3 km air than environmental air from farther aloft, it is colored by the most prevalent tracer in the grid box.

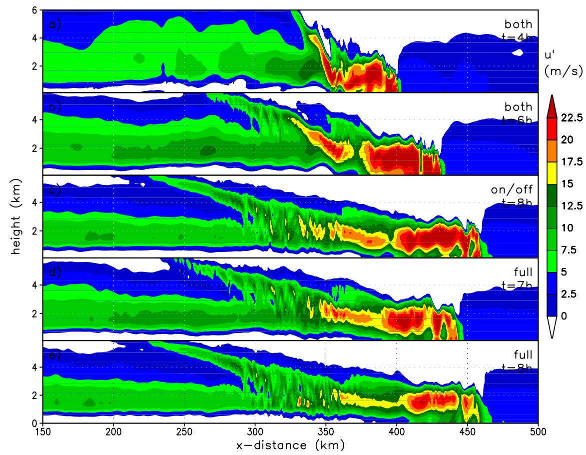

Figure 7: Cross section of rear–to–fore wind perturbations (shaded as shown). a) for both the full and on/off cooling runs (they are identical) at t=4h, b) for both the full and on/off cooling runs (they are identical) at t=6h, c) for the on/off cooling run at t=8h, d) for the full cooling run at t=7h, e) for the full cooling run at t=8h.

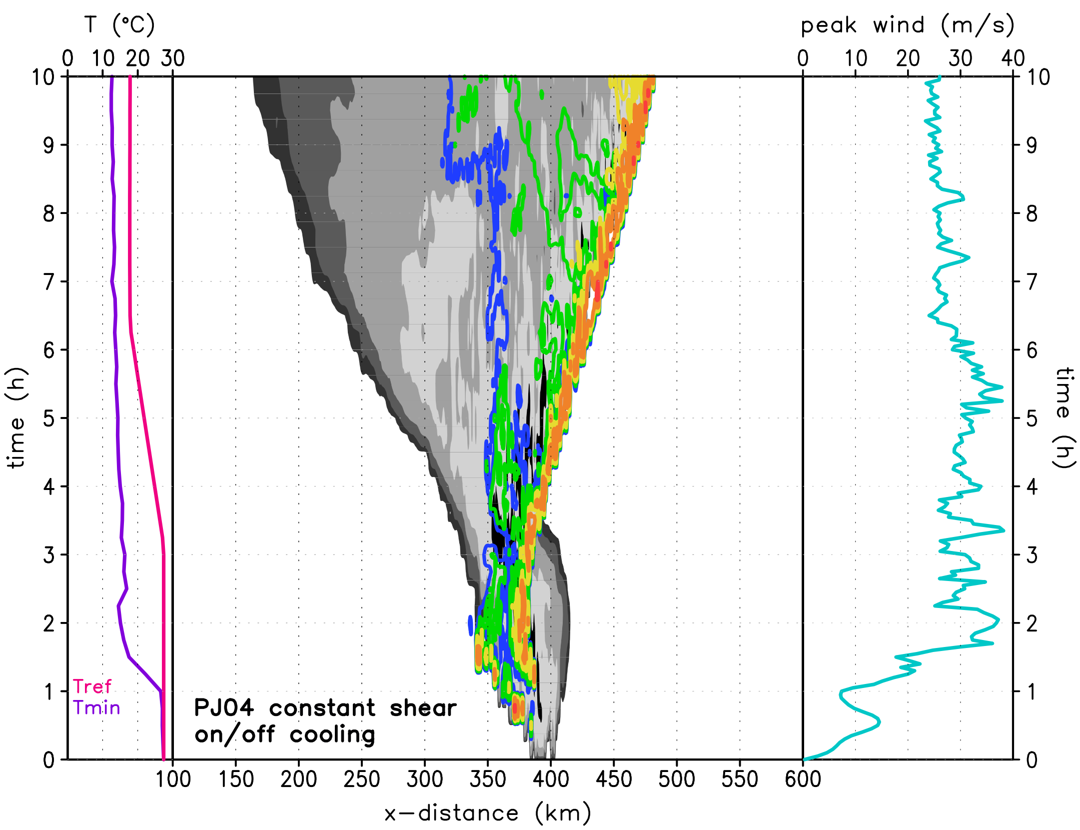

Figure 8: Same as Fig. 2 except for the run in which the 3 K h^{-1} cooling was begun at t=3h but ceased when T_{ref}=291 K. Note that 10 hours are depicted (vs. 8h in Fig. 2).